Ab initio study of linear atomic chains in copper nanowires

E. P. M. Amorim and E. Z. da Silva
Institute of Physics "Gleb Wataghin," University of Campinas–Unicamp, 13083-970 Campinas, SP, Brazil
(Received 17 September 2009; revised manuscript received 17 December 2009; published 31 March 2010)

Recently experimental and theoretical results established that copper nanowires (NWs) evolve to form linear atomic chains when pulled along the [100], [110], and [111] crystallographic directions. Since that, copper NWs became an exciting alternative to produce nanocontacts. In the present study, we used *ab initio* calculations based on density-functional theory within the local density and generalized gradient approximations to investigate the electronic structure of copper NWs obtained from previous tight-binding molecular dynamics (TBMD) simulations. The TBMD structures obtained just before rupture were used for the *ab initio* calculations. By pulling the NWs quasistatically in these cases, we also observed their breaking at similar distances as in the TBMD, regardless of the exchange-correlation potential used. The pulling forces before rupture were also presented for TBMD and *ab initio* calculations and they are in good agreement. Finally, we present a detailed analysis of the electronic structure of selected atoms from the NWs linear atomic chains and tips before rupture. Our results show that the electronic properties are bulklike for atoms with coordination six or more. However, lower coordinated atoms from tips and linear atomic chains have their electronic properties characterized by sharper *d* and *s* states shifted toward the Fermi energy.

DOI: 10.1103/PhysRevB.81.115463 PACS number(s): 61.46.−w, 62.25.−g, 71.15.Pd, 73.22.−f

I. INTRODUCTION

The search to increase the computational processing capability produced intense scientific and technological efforts to make electronic circuits smaller and more efficient, consolidating the molecular electronic or nanoelectronic age. In this context, the investigation of mechanical properties, electronic structure, and charge transport in metallic nanowires (NWs) became of fundamental importance, since under stretching conditions, some NWs evolve to form linear atomic chains (LACs), the smallest conductors possible, which could be used to make electric contacts to connect nanodevices.

In the nanoscale, there are new and interesting effects due to the quantum nature of the materials. Some mechanical properties are quite unusual and differ from what is observed in bulk. For example, a nanoconductor response to applied stress through structural rearrangements and its yield strength can be one or two orders of magnitude larger than its bulk counterparts.[1] Weird structures with multishell, helical, or tubular shape are predicted theoretically[2–5] for many metals and observed experimentally for gold[6,7] and platinum.[8] For copper nanowires, currently there is no experimental evidences showing weird structures. However, theoretical work such as molecular dynamics (MD) with empirical many-body potential[9,10] and a method derived from density-functional theory (DFT) calculations[11] studied multishell NW possibilities. Tight-binding MD calculations parameterized from *ab initio* results[12] compared the behavior copper and gold single wall NWs. The present simulation did not find helical formation for the NWs studied. Other works studied the formation of atomic chains and the relation between mechanical and electronic properties using similar theoretical frameworks as the ones used here for other metals[13,14] evidencing the intense search for different nanocontacts.

Charge transport in quantum-size conductors occurs ballistically in quantized units ($1G_0=2e^2/h$) of conductance and is strongly dependent on structural arrangement of the atoms.[1] Mechanically controlled break junction technique[15–20] or pulling atoms with a scanning tunneling microscope (STM) tip which is brought into contact with a flat metal surface[21,22] can be used to produce atomic point contacts. The conductance measurements across a copper atom point contact exhibit a clear plateau about $1G_0$.[15–22] Stable copper NWs were obtained by electrochemical deposition of copper between a gold electrode and a sharp STM tip[23] and presented the same result encountered above. Producing holes in a copper thin foil with a high-resolution transmission electron microscope (HRTEM) and decreasing the electron beam intensity to image acquisition, it was possible to follow the dynamical evolution of copper NWs until the rupture.[20] Such experiment evidenced the existence of atomic chains formed in copper NWs along the [100], [110], and [111] crystallographic directions.

All these experimental results for metal NWs and, in particular, copper NWs motivated us to theoretically study these systems. We used both tight-binding molecular dynamics (TBMD) and DFT electronic-structure calculations to investigate the mechanical properties and electronic structure of copper NWs. The work is presented in two parts, in Sec. II we discuss the TBMD evolution of these NWs under stress along the [100], [110], and [111] growth directions that formed tips which evolved to LACs, all the way until their rupture.[24] In Sec. III we used *ab initio* DFT based SIESTA code to study the final stages of the evolution of these structures. We used structures from the final stages of the previous TBMD calculations, as inputs for DFT quasistatic evolution under stress, all the way until they ruptured, studying in detail their mechanical and electronic properties. Two approximations for the exchange-correlation functionals were considered, local density (LDA) and generalized gradient (GGA). We also compared the TBMD results with the *ab initio* ones to verify the quality of our TBMD calculations.

II. TIGHT-BINDING MOLECULAR DYNAMICS SIMULATIONS

The study of copper NWs under stress until rupture have been useful to obtain information of mechanical properties such as force profile under tension and to observe the LAC formation.[24] These properties are very important to determine the possibility to use copper NWs as nanocontacts. For this purpose, the TBMD is a reasonable choice since it is a total-energy method which situates itself between empirical and *ab initio* methods in terms of computational cost. It is more accurate than empirical methods because it includes the electronic structure using a set of parameters obtained via fully *ab initio* linear augmented plane wave (LAPW) method calculations[25] and calculates the quantum-mechanical forces. For these reasons, the low computational cost of TBMD compared to *ab initio* methods allows us to perform dynamical simulations of the order of hundreds of picoseconds of simulation time at finite temperatures.

The tight-binding (TB) parameters were calculated for many materials and in different structures to guarantee high transferability. For example, the parametrization of molybdenum was made to fit the total energies and band structure for four volumes in the fcc structure and five volumes in the bcc structure.[25] Using these TB parameters to determine the lowest-energy structure Mehl and Papaconstantopoulos found the structure called α-Mn with 29 atoms, a structure not included in the parametrization. For noncrystalline cases, TB parameters for gold and copper were used in TBMD calculations to study the liquid phase of gold,[26] gold NWs,[4,27,28] and copper NWs (Ref. 24) with good agreement with *ab initio* and experimental results.

We performed TBMD calculations of copper NWs stretched along the [100], [110], and [111] crystallographic directions.[24] The simulation protocol followed four steps: (i) initial annealing from 400 K until temperatures below 50 K in 4, 10, and 5 ps with damping parameter of 0.001, 0.0005, and 0.001 fs^{-1}, respectively, to [100], [110], and [111] NWs to obtain more stable structures. These structures have a initial elongation along the stretching direction varying from 1.2% to 2.5% compared to the bulk structure. (ii) These NWs were elongated by 0.40, 0.35, and 0.50 Å and the temperature was set at 400 K. (iii) New annealing done in 2, 5, and 3 ps for [100], [110], and [111] NWs. (iv) Steps (ii) and (iii) were repeated until the NW breaking. The equations of motion were integrated using the Verlet algorithm and Brillouin-zone sampling was done using the Γ point. The supercell dimensions were chosen to avoid the interaction between the NWs and their images.

Figure 1 shows the initial structures in two perspectives, after the first relaxation and before the rupture for copper NWs stretched along the [100], [110], and [111] crystallographic directions.[24] The NW along the [100] direction shown in (a) was assembled with (i) four series of two planes with 12 and nine atoms repeated stacking to a total of 84 atoms. After the first annealing the structure was partially relaxed as can be seen in a-ii. The structure a-iii shows the NW close to rupture, displaying two pyramidal tips with a LAC of three atoms with its bond distances and the arrow indicating the bond that ruptured. The second NW, structure

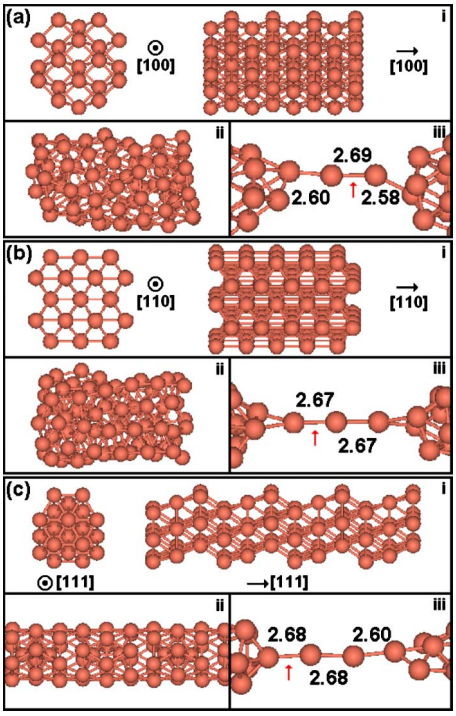

FIG. 1. (Color online) Dynamical evolution of (a) [100], (b) [110], and (c) [111] copper NWs. Frame (i) gives the initial structures, (ii) the first relaxation, and (iii) structures before the rupture. The red (gray) arrow indicates the ruptured bond.

(b) was stretched along the [110] and it was constructed with eight and nine atoms per plane with these two planes repeated five times to form a NW with 85 atoms (b-i). Frame b-ii shows the structure obtained after the first annealing and frame b-iii depicts the final structure with a LAC of three atoms. The third NW, structure (c) was made as a series of three planes with seven, six, and seven atoms repeated four times, to a total of 80 atoms (c-i). In frame c-ii the [111] NW exhibited a strong tendency to expose a closed-packed surface as in the case of gold NWs (Refs. 12, 27, and 28) showing a folded (111) sheet. This NW was the only one which totally relaxed after the first annealing. The LAC with four atoms (c-iii) is the largest LAC of all structures studied. A more detailed discussion about these calculations, details of how the one atom constrictions were formed, how they evolved to form LACs and force profiles were discussed in Ref. 24. The results presented in this section are important since some selected TBMD structures were used as inputs to the present *ab initio* study and also TBMD and *ab initio* results are compared in the next section.

III. *AB INITIO* CALCULATIONS

Copper NWs produced by the TBMD simulations showed a varied and rich set of structures and a further study of their mechanical and electronic properties is a matter of interest to better understand their behavior and to access the possibility of use them in applications. In order to get a better understanding of the electronic structure in these extremely unusual atomic arrangements where copper forms NWs with

TABLE I. Lattice parameter (a), bulk modulus (B), and cohesive energy (E_C) calculated for bulk cooper, and bond length (l) and bond energy (E_B) for copper dimer.

	LDA[a]	LDA	GGA	Exp.[b]
a (Å)	3.58	3.58	3.67	3.60
B (GPa)	167	155	156	137
E_C (eV)	5.35	5.09	5.15	3.49
1 (Å)	2.17	2.17	2.18	2.22
E_B (eV)	3.21	3.06	3.16	2.01

[a]Using the basis optimized for bulk, see Ref. 38.
[b]For bulk information, see Ref. 39 and for dimer see Ref. 40.

tips and LACs showing coordination numbers and bond angles away from what they experience in bulk, we study the NWs produced from the TBMD calculations using an *ab initio* framework. The coordination numbers varied from 2 to 4 (LAC and tips atoms) until 6 or more (atoms at the NW surface or into the NW) with many possibilities of bond angles. The mechanical rearrangement of low-coordination atoms is strongly dependent on the chemical bonds, which are characterized by sharper *d* and *s* states that shifted toward the Fermi energy for *d*-metals such as gold,[5,28,29] copper, and silver.[29]

Our presentation of *ab initio* results is divided in three parts. First, we present technical details about the simulation protocols and some calculations for bulk and dimer to verify the quality of the pseudopotential used. In the second part, we analyze some mechanical properties as LAC lengths under stress and forces before the NW's rupture. The last section is devoted to the electronic structure and its relation to the different obtained structures.

A. Simulation protocols and preliminary calculations

We performed *ab initio* total-energy calculations based on DFT (Refs. 30 and 31) using TBMD structures before the rupture shown in Fig. 1 as inputs. Norm-conserving Troullier-Martins pseudopotentials[32] with nonlocal partial-core corrections[33] were used to describe the interaction between valence and core electrons. The exchange-correlation functionals considered were LDA (Ref. 34) and GGA.[35] These calculations were performed using the SIESTA code.[36] The basis sets were described with a split valence double-zeta basis (spin polarized) and localized numerical orbitals were used with a confining energy of 0.08 and 0.18 eV for LDA and GGA, respectively. The grid integration to represent the charge density was defined with a cutoff of 200 and 300 Ry (LDA and GGA, respectively) to perform the conjugate-gradient (CG) evolution. The grid of 400 Ry was used to obtain the density of states for the structures before rupture for both exchange-correlation approximations. Supercells were defined with periodic-boundary conditions to define the chain geometries and to avoid interactions between the NWs with their images. The Brillouin-zone sampling was represented by eight *k* points along the NW axis.[37]

Table I shows some calculations performed for the bulk and dimer of copper to check the parameters and the pseudopotential used. The first column presents calculated results using a basis optimized to the bulk[38] (LDA), the second and third columns give our LDA and GGA calculations using the energy shifts mentioned above. These results show a deviation between calculated values and experimental results up to 2% for bulk lattice parameter and dimer bond length and around 13% for the bulk modulus. The cohesive and bond energies have considerable deviations about 50% and 60% from the experimental value but compatible with other theoretical results.[40]

The CG method was used to relax the forces to reach minimal-energy structural configurations. This method was chosen for the *ab initio* calculations since it shows the fastest convergence than other methods such as steepest descent or simulated annealing.[41] The relaxation was done until all force components were smaller than 0.01 eV/Å. The procedure to evolve the copper NWs until the rupture followed three steps: (i) perform a CG calculation for the initial configuration, the structure from TBMD before the rupture, (ii) increase the NW along the stretching axis by 0.1 Å, (iii) new CG calculation performed from the stretched configuration, and (iv) repeat the steps (ii) and (iii) until the observation of tip retraction or a sudden increase of one bond indicating the NW rupture. These calculations were performed for copper NWs stretched along the directions previously studied using TBMD. They are the subject of the next section where we also analyze in more detail the rupture, calculate forces and compare them with our previous TBMD results.

B. Mechanical properties

Metallic NWs support tension during the stretching process, increasing the sustained forces linearly until a rearrangement occurs, reducing the tension. At such events, there is an abrupt reduction in the sustained forces, then they increase linearly from small values until a new rearrangement occurs, repeating this process. This is the so-called sawtooth behavior of the forces until rupture.[24,28] After some rearrangements, the NWs evolve to a one-atom constriction which indicate the beginning of the LAC formation. The evolution of the LAC continues with these rearrangements and inclusion of atoms from the tips into the LAC, until the tips reach symmetrical configurations. At this point, the tension causes the increase in the distance between atoms in the LAC due to their low coordination since they have less resistance to support tension than the atoms from the tips or the bulk, therefore the LAC bonds increase almost linearly until the rupture.[24]

The breaking process in copper NWs occurred after the LAC formation as presented in the TBMD study and to get a better insight about when and how the rupture occurs, we performed a simple calculation considering a linear trimer (LT), the typical LAC configuration of copper NWs under tension, to evidence the instability that occurs during the breaking process. We evaluated the LT potential energy curves varying the position of the central atom for different values of LT distance, to establish a critical LAC length for the breaking process.[42] Figure 2 shows the potential energy surface (PES) profile for a LT where the two external atoms

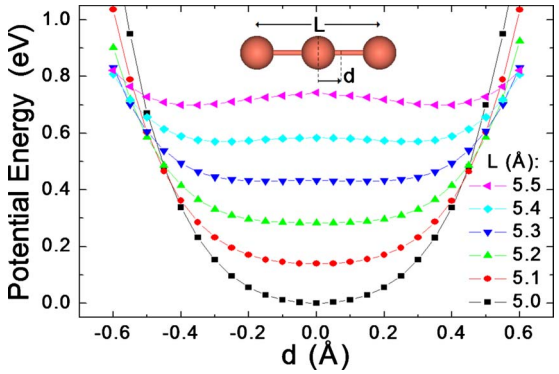

FIG. 2. (Color online) PES curves for some values of L (LAC length) versus the displacement of the middle atom.

were kept fix and the central atom was moved, for triplet lengths L from 5.0 to 5.5 Å using LDA. The PES evolution has two contrasting configurations as function of L. Small values of L give a stable one minimum with the central atom favoring the stable central position with equal bond lengths. Beyond a critical L value, the PES evolved to a two minima profile. The onset of the instability, transformed the stable central position into a maximum that became unstable. In these cases, the atom has to choose one of the minima causing the breaking of the structure since the other bond gets too large. This analysis revealed one minimum for L values from 5.0 to 5.2 Å, showing a stable LAC with the central copper atom favoring the central position. On the other hand, LAC lengths from 5.3 Å developed a two minima profile. However, the energy difference between the central position and the two minima for L values 5.3 and 5.4 Å are about 1.1 and 1.3 meV and are displaced from the middle position by ± 0.15 and ± 0.30 Å, respectively. Although, the potential barriers are so small in both cases, the presence of two minima is one indication of an unstable LAC, therefore the bonds close to the rupture should be for values in the range 2.65–2.70 Å. The last case, namely, $L=5.5$ Å the average bond was 2.75 Å and the potential barrier had grown enormously to 43 meV with the displacement minima going to ± 0.35 Å evidencing a break situation. We therefore argue that whenever a given LAC triplet gets larger than 5.3 Å the NW tends to break.

Probably in experiments at finite temperatures, bond distances at break tend to be smaller than the bonds considered in this quasistatic approach, due to thermal fluctuations, as shown in the case of gold NWs, where *ab initio* MD at finite temperatures[42] showed good agreement with experimental results.[43] Another interesting possibility in metal NW LAC formation is the effect of light impurities not observed in electron-microscopy experiments, they could explain some larger bond distances observed in the HRTEM images. From the theoretical point of view this possibility was investigated in gold NWs for many authors[42,44–47] and it is the subject of our current research for copper NWs.

The *ab initio* electronic structure calculations for the evolution of the copper NWs under stress starting from the previous TBMD structures for elongations just before the breaking were done using both exchange-correlation approximations (LDA and GGA). The first CG steps using

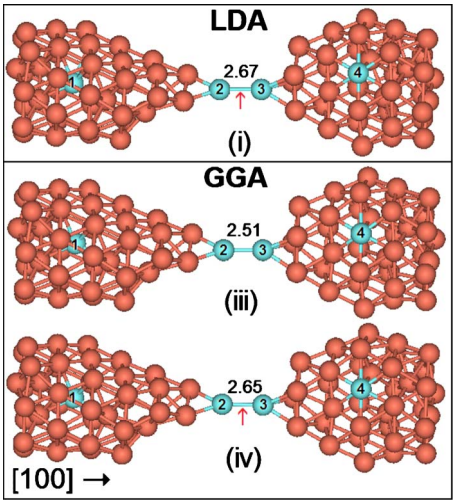

FIG. 3. (Color online) Copper NW stretched along [100]: (i) after the first CG performed on the TBMD structure (from Fig. 1) obtained using LDA and (iii) after the first CG performed on the LDA structures (i) and (iv) after stretching and before the rupture using GGA. The red (gray) arrows show the breaking bond.

GGA showed a tendency to increase the NW volume, like a inflating process which compressed the LACs that became shorter and also showed a zigzag form, evidencing larger bond distances calculated using GGA than those obtained using LDA. Zigzag configurations were obtained previously for gold[28] and this difference between bonds from the bulk parts of NWs is consistent with the fact that the bulk lattice parameter calculated using GGA was 3.5% larger than LDA calculation, as can be seen in Table I. Therefore, the presentation of Figs. 3–5 showing copper NWs stretched along the [100], [110], and [111] directions have the following order: (i) structures from the TBMD simulation, obtained after the first CG *ab initio* relaxation using LDA; (ii) the last structures before the NWs break, also using LDA; (iii) structures obtained after a CG relaxation from the structures obtained in (i) using GGA, and (iv) the final GGA structure obtained before the NW break. Some atoms in blue (light gray) and numbered from 1 to 4 with different coordination were chosen for the investigation of their electronic structure as discussed in the next section.

Figure 3 shows the evolution of the NW stretched along the [100] direction. Figure 3(i) has the initial LDA structure identical to the final structure, therefore the structure (i) is identical to (ii) in this case, before the rupture, since the NW breaks after the first CG relaxation. One atom from the LAC was incorporated back to the tip after the CG relaxation. The LAC reconstruction incorporating atoms back to the tip is a likely event in the case of very small LACs and has occurred in this case due also to the bulk bipyramidal structures that inflated compressing the short LAC. This NW had three atoms in the LAC in the final stages from TBMD and just two atoms from the tips in the structures obtained for both exchange-correlation approximations. The structure 3(i) has tips with a pyramidal shape with breaking bond distance before the rupture of 2.67 Å. From this configuration, after a CG relaxation using GGA, we can see this tendency to GGA bonds to be larger than the LDA ones. The only bond from

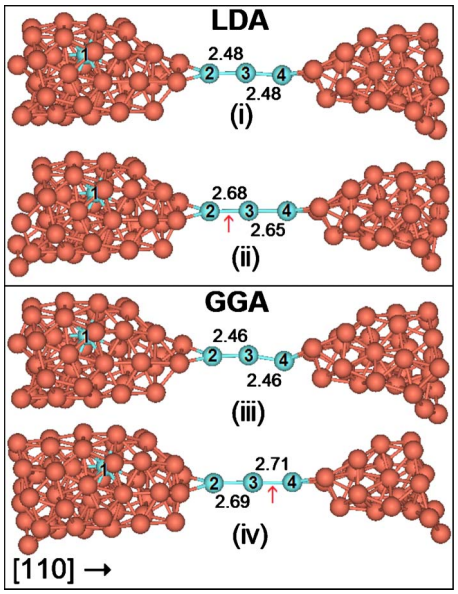

FIG. 4. (Color online) Copper NW stretched along [110]: (i) and (iii) after the first CG performed on the TBMD structure (from Fig. 1) obtained using LDA and GGA and (ii) and (iv) after stretching and before the rupture using LDA and GGA. The red (gray) arrows show the breaking bond.

the LAC was pressed by the tips and bulk parts decreasing its distance in 6% as showed in Fig. 3(iii). After stretching, this bond distance increased from 2.51 to 2.65 Å in Fig. 3(iv) becoming a breaking bond as the LDA one in Fig. 3(i). These breaking bonds calculated here are almost 1% and 1.5% smaller than the TBMD one for LDA and GGA calculations.

Figure 4 shows the NW stretched along the [110] direction. After a first CG relaxation the LAC displays three atoms [Figs. 4(i) and Fig. 4(iii)] as the previous TBMD structure (Fig. 1). In these cases, the LAC bonds are very similar, in good agreement with the trimer discussed previously,

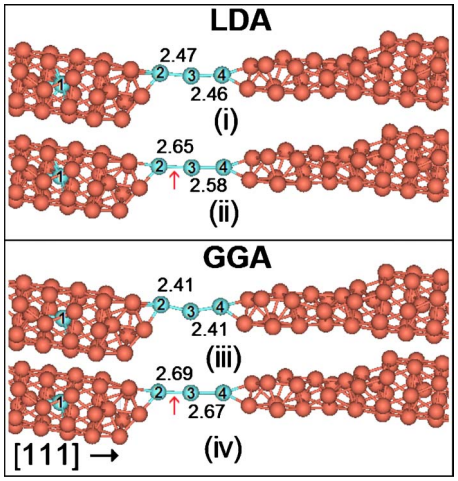

FIG. 5. (Color online) Copper NW stretched along [111]: (i) and (iii) after the first CG performed on the TBMD structure (from Fig. 1) obtained using LDA and GGA and (ii) and (iv) after stretching and before the rupture using LDA and GGA. The red (gray) arrows show the breaking bond.

TABLE II. Forces (nN) before the rupture for all calculations.

Direction	TBMD[a]	LDA	GGA
100	2.0	1.8	1.8
110	1.5	2.1	2.3
111	1.6	2.4	2.0

[a]From Ref. 24.

where the central atom is in a symmetrical position with respect to its neighbors for trimer lengths smaller than 5.2 Å (Fig. 2). However, the LAC is under compression because tip atoms are pushing the LAC making the bonds almost linear with angle 176° for LDA [Fig. 4(i)] and zigzag with angle 169° for GGA [Fig. 4(iii)] but with almost equal distances. Upon further stretching, the NW evolved and bond distances before rupture were similar to the TBMD (Fig. 1) for the LDA calculation in Fig. 4(ii) and about 1% larger for the GGA showed in Fig. 4(iv), also in this case, the breaking bond occurred for the bond 2–3 for LDA and for the bond 3–4 for GGA approximation.

The NW stretched along the [111] direction is presented in Fig. 5. The first difference compared to the TBMD calculation is the number of atoms which decreased from four to three atoms. After the first CG performed from the TBMD calculation, the LAC had symmetrical bonds and its bonds were almost linear with angles of 173° and 158° as showed in Figs. 5(i) and Fig. 5(iii) (LDA and GGA) similar to the last case showed above. After the stretching, the average bond before rupture was almost 1.5% smaller for LDA Fig. 5(ii) and 1% larger for GGA Fig. 5(iv) as compared to TBMD, showing a good agreement with the cases above. In this case, the breaking bonds were the same for both exchange-correlation approximations and for [110] and [111] cases, they occurred for trimer distances larger than the critical instability value L_C=5.3 Å.

Table II displays the forces before rupture for all cases comparing them with previous TBMD results. The *ab initio* forces gave values from 1.8 to 2.4 nN while the TBMD forces were from 1.5 to 2.0 nN, showing a reasonable agreement between them, similar to the agreement obtained in the case of gold NW.[5]

The structure of the NWs shown here are qualitatively similar to the TBMD counterparts: a bipyramidal shape for the [100] tips and rodlike for the [110] and [111] directions. The number of atoms in the LAC, on the other hand changed in the [100] and [111] cases and bonds were slightly larger than the TBMD ones. Copper NWs have shorter LACs and are less malleable[12] than gold NWs, in which cases no major reconstruction were observed in comparison between TBMD and *ab initio* calculations.[28] The stretching processes were performed without temperature in small stretching steps of 0.1 Å as explained above, differently from the annealing process used in TBMD, however as we can see, the bond-breaking distances are in good agreement between *ab initio* and TBMD calculations having a maximum difference of about 1.5%. The next section presents the electronic structure of these copper NWs relating them with the structural properties discussed here.

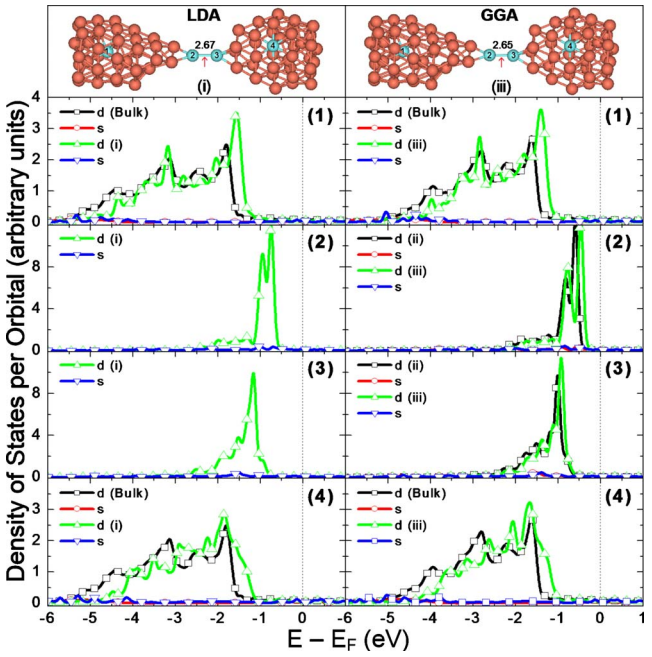

FIG. 6. (Color online) Density of states for copper NW stretched along the [100] direction calculated using LDA and GGA. The index (ii) refers to the structure in Fig. 3.

C. Electronic structure

The understanding of the electronic structure and its relation with the mechanical properties in a nanoconductor is a fundamental issue to access the possibility of use it in devices or electric contacts. Copper, is a transition *d* metal which in bulk has a face-centered cubic structure with 12 first neighbors and density of states profile for *d* orbitals characterized by an energy distribution in the interval −6 to −1 eV bellow the Fermi level. When the coordination number decreases, this electronic distribution changes becoming sharper and shifted toward the Fermi level. However, as will be shown, for six or more coordinated atoms, the density of states is very similar to the bulk (bulklike) while for lesser coordinated atoms an unusual behavior emerges. This occurs in the case of atoms from the tips and LACs, as they are two to four coordinated. Figures 6 and 7 display the projected density of states (PDOS) per orbital for all copper NWs presented above, after the first CG relaxation (as in Figs. 3–5) and before rupture when the LAC is a straight line (Figs. 3–5 and also on Figs. 6 and 7). Selected atoms labeled from 1–4 were chosen for the electronic structure study due to their distinct coordinations, as representative examples of typical coordination encountered in these metallic NWs. For bulklike atoms, we compare them with bulk copper.

The density of valence states projected per orbital was calculated using LDA (left) and GGA (right) for the copper NW stretched along the [100] direction and displayed in Fig. 6. Atom (1) is deep inside the pyramidal tip and it is surrounded by ten and nine atoms (LDA and GGA). The PDOS for this atom is bulklike as can be observed by its similarity to bulk copper even so bond distances and bond angles were different than in bulk. Another similar situation could be observed with atom (4) which is a surface atom bounded to six atoms from the surface and to another one inside the NW, also as bulklike. These atoms are bulklike, however they have a shy shift to the Fermi level and these cases are quite similar for both exchange-correlation approximations. On the other hand, atoms (2) and (3) are three- and four-coordinated, respectively, and their densities of states are characterized by sharper states localized in two peaks for atom (2) and just one for atom (3) shifted toward the Fermi

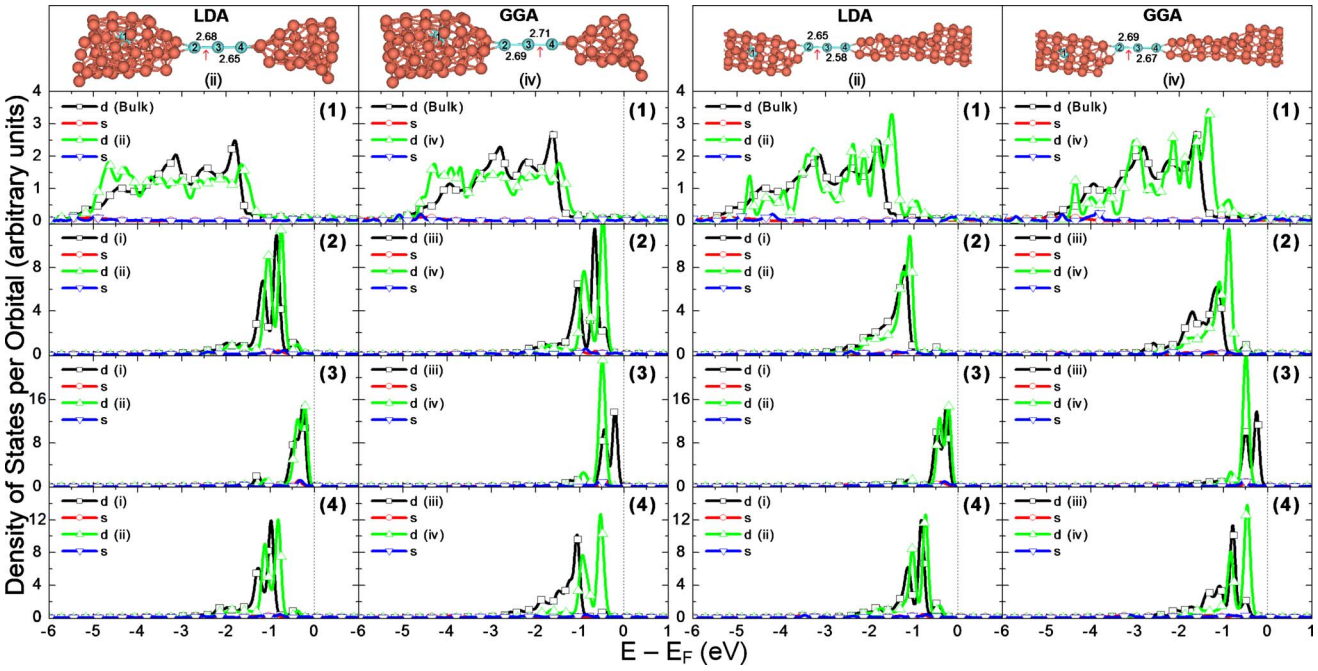

FIG. 7. (Color online) Density of states of copper NW stretched along the [110] (left) and [111] (right) directions calculated using LDA and GGA. The indices (i) and (iii) refer to the structures in Figs. 4 and 5.

level with some differences between LDA and GGA calculations. The structures (i) and (iii) have bond distances very similar for both exchange-correlation approximations. In the GGA case, we observed a peak shift of about 0.3 eV toward the Fermi level, as the structure evolved from (ii) to (iii) caused by the increase in bond distance exhibiting also sharper peaks. The shift in energy of the DOS toward the Fermi level considering the change in coordination, reveals that the effect of reduction in the number of neighbors from the bulk value to nine or ten atoms (atom 1) or seven atoms (atom 4) is less intense compared to the shift to the Fermi level for three- or four-coordinated atoms. Besides this, all peaks are closer to the Fermi level in GGA than in LDA for both *d* and *s* states.

Figure 7 depicts densities of states for copper NWs stretched along the [110] (left) and [111] (right) directions. First, let us focus on the [110] NW. Atom (1) is surrounded by 11 and ten atoms for LDA and GGA, respectively, and its PDOS shows an almost bulklike behavior but with small differences when compared with the bulk density of states. The bonds around atom (1) are smaller than the bulklike atoms inside the NW from the [100] and [111] copper NWs. The surface of this NW is formed by rings which have an angle with the stretching direction, similar to the [110] gold NW.[5] The distances and angles between atom (1) and its neighbors are different from the bulk. Although some differences exist, there are also similarities between the atom (1) PDOS and bulklike behavior: it keeps some bulk characteristics such as energy width and same height in the density of states. Atom (2) is three-coordinated and it has two distinguish peaks, as the atom (2) in the [100] copper NW and also more shifted to the Fermi level in GGA than in LDA for the *d* state. The *s* state, exhibits a sharper peak in GGA than in LDA which is centered about 1 eV bellow the Fermi level. Atom (3) in the center of the LAC has coordination 2 and in this case, the GGA approximation shows one peak sharper and about 50% higher than the LDA one. Both peaks are centered around the value −0.5 eV and also very close to the Fermi level. Other interesting fact is the localization of the *s* state centered in the same energy value of the *d* state. The *s* state is associated to the electronic transport in *d* metals. In this case, both states are very close to the Fermi level and with peaks in the same energy. This could bring new features to the transport in this NW. Atom (4) is also three-coordinated and it has an electronic structure very similar to atom (2) just discussed, without qualitatively differences between LDA and GGA calculations before rupture. Comparing the structural changes from structures (i) to (ii) in LDA with the change in the PDOS profile, we can see a shift about 0.3 eV while the GGA case from (iii) to (iv) shows a larger shift. Qualitatively, besides the shift, there are no differences between the structure (i) to (ii) in LDA for the atoms (2)–(4). On the other hand, for atom (3) in GGA, the structure (iii) displayed two distinct peaks that evolved to a single sharper peak around 0.5 eV below the Fermi level (structure iv). In the case of atom (4) the difference in DOS for LDA and GGA as the structure evolves is caused by structural the form of the LAC that in the LDA case from (i) to (ii) is almost linear, so only a shift is observed in the DOS, while the GGA starts as zigzag (iii) that evolves to an almost linear form in (iv). The GGA is an approximation in which, the effect of gradient of the charge density is well described, therefore should be better to address the local environment. Since the structural differences between structure (iii) to (iv), respectively, to atoms (3) and (4) are related to the bond angles and distances, the differences regarding the PDOS could be better described using GGA approximation.

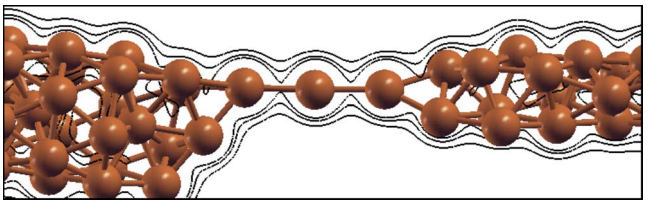

FIG. 8. (Color online) Charge-density isolines of [111] copper NW calculated using GGA.

Now, our focus is the density of states of [111] copper NW on the right side of the Fig. 7. This NW evolves to a LAC with three atoms as the [110] showed above. In this case, LAC distances are larger for GGA than LDA calculations. In this case, the NW has a closed-packed structure which is mentioned in other works for copper[12,24] and also for gold[12,27] stretched in the same direction. This structure is a tube which is a folded (111) sheet and the inside atoms are surrounded by the surface rings with six atoms. The inside trapped atoms form dimers. Although, the dimer is trapped inside this structure, the distances between the rings and the inside atoms are bit larger than the average distance observed in bulk but the distance to the other inside atom is shorter than the bulk and larger than the copper dimer. Apart from these differences, atom (1) has a density of states very similar to the bulk, thus it is bulklike and also shifted to the Fermi level as the previous cases. Atom (3) in the center of the LAC has strong localized *d* and *s* states at the same energy similarly as observed in [110] copper NW. The discussion about the evolution of structures from (i) to (ii) and from (iii) to (iv) are compatible with the previous discussion for the [110] copper NW.

In order to give some insight on the spatial charge distribution of copper NWs, Fig. 8 presents three sets of charge-density isolines[48] for values 0.005, 0.010, and 0.015 electrons/(Bohr)^3 of the [111] copper NW in a plane that contains all the atoms from the LAC evidencing a metallic delocalized bond as obtained previously in the case of a gold NW.[28] These configurations were calculated for LDA and GGA and both cases are very similar, therefore we only present the GGA plot.

IV. CONCLUSIONS

In this work, we studied electronic and structural properties of thin copper NWs. The work compared previous results obtained using TBMD with *ab initio* results showing a good agreement between them for the linear atomic chain distances and forces before rupture of the NWs. We have also studied the electronic structure of these copper NWs for all final structures using LDA and GGA approximations with

a discussion about similarities and differences between these approximations. Our results showed that the densities of states are bulklike for atoms with coordination six or more, at the NW surface or inside the NW's tip. For lower coordinated atoms, coordination varying from two to four atoms, *d* states are localized and shifted toward to the Fermi level. In these cases, the GGA calculations gave more localized and sharper results than LDA and also more shifted toward the Fermi level. The atoms from the center of LACs, bounded to other two atoms, also revealed localized *s* states in the same energy of the localized *d* states around the Fermi level which could be interesting for further analysis in transport calculations. The GGA approximation revealed to be sensitive to the bond angles and distances exhibiting sharper peaks for low coordinated atoms compared to LDA. Finally, the density of charge revealed delocalized metallic bonding.

ACKNOWLEDGMENTS

We would like to thank Rodrigo Yoshikawa Oeiras for fruitful discussions about *ab initio* calculations. The TBMD developed by F. Kirchhoff as part of the Computational Chemistry and Materials Science Computational Technology Area (CCM CTA)'s a U.S. Department of Defense CHSSI program. The simulations were performed at the CENAPAD-SP and IFGW-Unicamp. We acknowledge support from FAPESP and CNPq. E.P.M.A. was supported by CAPES.

[1] N. Agraït, A. L. Yeyati, and J. M. van Ruitenbeek, Phys. Rep. **377**, 81 (2003).
[2] O. Gülseren, F. Ercolessi, and E. Tosatti, Phys. Rev. Lett. **80**, 3775 (1998).
[3] E. Tosatti, S. Prestipino, S. Kostlmeier, A. Dal Corso, and F. D. Di Tolla, Science **291**, 288 (2001).
[4] Y. Iguchi, T. Hoshi, and T. Fujiwara, Phys. Rev. Lett. **99**, 125507 (2007).
[5] E. P. M. Amorim and E. Z. da Silva, Phys. Rev. Lett. **101**, 125502 (2008).
[6] Y. Kondo and K. Takayanagi, Science **289**, 606 (2000).
[7] Y. Oshima, A. Onga, and K. Takayanagi, Phys. Rev. Lett. **91**, 205503 (2003).
[8] Y. Oshima, H. Koizumi, K. Mouri, H. Hirayama, K. Takayanagi, and Y. Kondo, Phys. Rev. B **65**, 121401(R) (2002).
[9] J. W. Kang and H. J. Hwang, J. Phys.: Condens. Matter **14**, 2629 (2002).
[10] J. W. Kang, J. J. Seo, and H. J. Hwang, J. Phys.: Condens. Matter **14**, 8997 (2002).
[11] B. Wang, J. Zhao, X. Chen, D. Shi, and G. Wang, Nanotechnology **17**, 3178 (2006).
[12] E. P. M. Amorim, A. J. R. da Silva, and E. Z. da Silva, J. Phys. Chem. C **112**, 15241 (2008).
[13] A. Monari, V. Vetere, G. L. Bendazzoli, S. Evangelisti, and B. Paulus, Chem. Phys. Lett. **465**, 102 (2008).
[14] A. Hasmy, L. Rincon, R. Hernandez, V. Mujica, M. Marquez, and C. Gonzalez, Phys. Rev. B **78**, 115409 (2008).
[15] J. M. Krans, C. J. Muller, I. K. Yanson, Th. C. M. Govaert, R. Hesper, and J. M. van Ruitenbeek, Phys. Rev. B **48**, 14721 (1993).
[16] J. M. Krans, J. M. van Ruitenbeek, V. V. Fisun, I. K. Yanson, and L. J. de Jongh, Nature (London) **375**, 767 (1995).
[17] C. J. Muller, J. M. Krans, T. N. Todorov, and M. A. Reed, Phys. Rev. B **53**, 1022 (1996).
[18] K. Hansen, E. Laegsgaard, I. Stensgaard, and F. Besenbacher, Phys. Rev. B **56**, 2208 (1997).
[19] B. Ludoph and J. M. van Ruitenbeek, Phys. Rev. B **61**, 2273 (2000).
[20] J. C. Gonzalez, V. Rodrigues, J. Bettini, L. G. C. Rego, A. R. Rocha, P. Z. Coura, S. O. Dantas, F. Sato, D. S. Galvao, and D. Ugarte, Phys. Rev. Lett. **93**, 126103 (2004).
[21] L. Olesen, E. Laegsgaard, I. Stensgaard, F. Besenbacher, J. Schiotz, P. Stoltze, K. W. Jacobsen, and J. K. Norskov, Phys. Rev. Lett. **72**, 2251 (1994).
[22] J. L. Costa-Krämer, N. Garci, P. Garcia-Mochales, and P. A. Serena, Surf. Sci. **342**, L1144 (1995).
[23] C. Z. Li and N. J. Tao, Appl. Phys. Lett. **72**, 894 (1998).
[24] E. P. M. Amorim, A. J. R. da Silva, A. Fazzio, and E. Z. da Silva, Nanotechnology **18**, 145701 (2007).
[25] M. J. Mehl and D. A. Papaconstantopoulos, Phys. Rev. B **54**, 4519 (1996).
[26] F. Kirchhoff, M. J. Mehl, N. I. Papanicolaou, D. A. Papaconstantopoulos, and F. S. Khan, Phys. Rev. B **63**, 195101 (2001).
[27] E. Z. da Silva, A. J. R. da Silva, and A. Fazzio, Phys. Rev. Lett. **87**, 256102 (2001).
[28] E. Z. da Silva, F. D. Novaes, A. J. R. da Silva, and A. Fazzio, Phys. Rev. B **69**, 115411 (2004).
[29] T. Nautiyal, S. J. Youn, and K. S. Kim, Phys. Rev. B **68**, 033407 (2003).
[30] P. Hohenberg and W. Kohn, Phys. Rev. **136**, B864 (1964).
[31] W. Kohn and L. J. Sham, Phys. Rev. **140**, A1133 (1965).
[32] N. Troullier and J. L. Martins, Phys. Rev. B **43**, 1993 (1991).
[33] S. G. Louie, S. Froyen, and M. L. Cohen, Phys. Rev. B **26**, 1738 (1982).
[34] D. M. Ceperley and B. J. Alder, Phys. Rev. Lett. **45**, 566 (1980).
[35] J. P. Perdew, K. Burke, and M. Ernzerhof, Phys. Rev. Lett. **77**, 3865 (1996).
[36] J. M. Soler, E. Artacho, J. D. Gale, A. García, J. Junquera, P. Ordejón, and D. Sánchez-Portal, J. Phys.: Condens. Matter **14**, 2745 (2002).
[37] H. J. Monkhorst and J. D. Pack, Phys. Rev. B **13**, 5188 (1976).
[38] J. Junquera, O. Paz, D. Sanchez-Portal, and E. Artacho, Phys. Rev. B **64**, 235111 (2001).
[39] C. Kittel, *Introduction to Solid State Physics* (Wiley, New York, 1986).
[40] E. M. Fernández, J. M. Soler, I. L. Garzon, and L. C. Balbas, Phys. Rev. B **70**, 165403 (2004).
[41] M. C. Payne, M. P. Teter, D. C. Allan, T. A. Arias, and J. D. Joannopoulos, Rev. Mod. Phys. **64**, 1045 (1992).
[42] E. Hobi, Jr., A. Fazzio, and A. J. R. da Silva, Phys. Rev. Lett. **100**, 056104 (2008).
[43] V. Rodrigues and D. Ugarte, Phys. Rev. B **63**, 073405 (2001).

[44] N. V. Skorodumova and S. I. Simak, Phys. Rev. B **67**, 121404(R) (2003).
[45] F. D. Novaes, A. J. R. da Silva, E. Z. da Silva, and A. Fazzio, Phys. Rev. Lett. **90**, 036101 (2003).
[46] E. Hobi, Jr., A. J. R. da Silva, F. D. Novaes, E. Z. da Silva, and A. Fazzio, Phys. Rev. Lett. **95**, 169601 (2005).
[47] F. D. Novaes, A. J. R. da Silva, A. Fazzio, and E. Z. da Silva, Appl. Phys. A: Mater. Sci. Process. **81**, 1551 (2005).
[48] A. Kokalj, Compt. Mater. Sci. **28**, 155 (2003); code available from http://www.xcrysden.org/